Available online at www.sciencedirect.com
ScienceDirect
Journal of Process Control 17 (2007) 333–347
JOURNAL OF PROCESS CONTROL
www.elsevier.com/locate/jprocont

Control of fuel cell power output

Federico Zenith, Sigurd Skogestad *

Department of Chemical Engineering, Norwegian University of Science and Technology, Sem Sælands veg 4, 7491 Trondheim, Norway

Received 12 May 2006; received in revised form 20 October 2006; accepted 22 October 2006

Abstract

A simplified dynamic model for fuel cells is developed, based on the concept of instantaneous characteristic, which is the set of values of current and voltage that a fuel cell can reach instantaneously. This is used to derive a theorem that indicates the conditions under which the power output of fuel cells can, in theory, be perfectly controlled. A fuel cell connected to a DC/DC converter is simulated numerically, with a control system based on switching rules in order to control the converter's output voltage. The resulting transients settle in about 5–10 ms. The converter is then used as an actuator in a cascade control loop to control the torque output of a DC electric motor with a PI controller in the external loop. In this loop, the resulting in transients settle in less than 0.2 s.

Keywords: Fuel cell; DC/DC converter; Electric motor

1. Introduction

Fuel cells are devices that convert chemical energy (often in the form of hydrogen) into electricity, without passing through a combustion stage. Whereas few fuel cell-based devices are currently available to consumers, they have the potential to be used, in different layouts and types, to provide electric power to utilities as diverse as cars, laptop computers, mobile phones, or even to the electric grid as a power station. Research in all of these areas is extensive, but dynamics and control of fuel cells have received comparatively less attention.

The focus of this paper is on controlling the power output delivered to an electric motor from a fuel cell through a DC/DC converter. This is currently the least studied aspect of control of fuel cells, but also one of its most important issues. In addition, control algorithms for flows, temperature and other variables may be needed, but these are outside the scope of the paper.

This work concerns also the choice of realistic manipulated variables for power control. In some papers, it is proposed to use feed flow rate to control power, but as discussed in the literature review this is not a good choice. A better strategy is to directly manipulate the power output to the external circuit. However, one cannot directly set the voltage or current as assumed in some of the literature, as these are actually determined by the connection of the fuel cell with the external circuit [1,2]. In this work, the strategy is to have the fuel cell connected to the external circuit only part of the time, by alternating a switch between ON and OFF in a DC/DC converter. This is also a common method to control power output from batteries. We chose to use a buck-boost converter, but other configurations are possible.

2. Literature review

2.1. Dynamics

Most dynamic models of fuel cells, such as for example in Amphlett et al. [3], normally consider current to be the system's input. Whereas this is legitimate in a dynamic model, it must be remembered that current is not a directly manipulable input variable: it is rather the control objective

* Corresponding author. Tel.: +47 73 59 41 54; fax: +47 73 59 40 80.
E-mail addresses: zenith@chemeng.ntnu.no (F. Zenith), skoge@chemeng.ntnu.no (S. Skogestad).

0959-1524/$ - see front matter © 2006 Elsevier Ltd. All rights reserved.
doi:10.1016/j.jprocont.2006.10.004

Nomenclature

C	capacitance (F)	R	resistance (Ω)
D	duty ratio (−)	T	torque (N m)
E	reversible potential (V)	V	voltage (V)
i	current density (A m^{-2})	Z	impedance (Ω)
I	current (A)	η	overvoltage (V)
L	inductance (H)	Φ	magnetic field (Wb)
P	power (W)	ω	angular velocity (rad s^{-1})

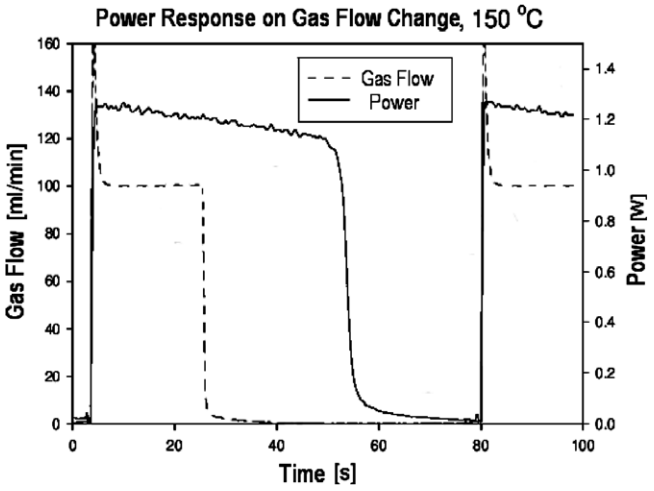

Fig. 1. Experimental data showing the delay in response from a step in reactant feed rate to a fuel cell's power output (from Johansen [13]).

than the means of control. Therefore, many models found in the literature will have to be adjusted to use manipulable inputs before they can be useful in a process-control setting. A proper means of control has to be clearly identified.

The model produced by Amphlett et al. [3] is essentially a thermal model with a basic, empirical modelling of the overvoltage effects. Cell current is considered a system input, and the catalytic overvoltage is assumed to vary instantly as a function of temperature, oxygen concentration and current. The model predicts well the behaviour of the stack in a time scale of minutes, but, since it does not treat the overvoltage as a state, it might be less accurate in the scale of seconds and lower.

Ceraolo et al. [4] developed a dynamic model of a PEM fuel cell that included the dynamic development of the catalytic overvoltage. Whereas they did not apply their results to control, they produced a model that could easily be modified for control applications; they also included a model for multicomponent diffusion on the cathode side, based on Stefan–Maxwell equations.

Pathapati et al. [5] produced a model that calculated the overvoltage as in Amphlett et al. [3], integrating the catalytic overvoltage and non-steady-state gas flow analysis.

Weydahl [6], who concentrated on experimental measurements of the electrochemical transient of PEM and alkaline fuel cells, measured transients in the range of 0.01–1 s.

2.2. Control

Two similar US patents have been granted to Lorenz et al. [7] and Mufford and Strasky [8], both concerning methods to control the power output of a fuel cell. Both these methods use air inflow as the input variable. Whereas this variable can indeed be set by manipulating the air-compressor speed, there are various reasons why this choice of input variable is not successful. First of all, only the fuel cells per se are considered: vital information is lost about the utility that will draw power from the cell. Also, while it could seem intuitive that a fuel cell will produce more power the more oxidant it is fed, this neglects a series of phenomena such as the mass-transport limit, the strong non-linear effects of oxygen partial pressure in the cathode kinetics, the diffusion of oxygen through the cathode and the accumulation of oxygen in the cathode manifold.

In the PhD thesis by Jay Pukrushpan [9] there is a lot about control of fuel cell systems, with focus on air-flow control and a large section about control and modelling of natural-gas fuel processors. Notwithstanding the high quality of the work, Pukrushpan has seemingly misquoted another author, Lino Guzzella [10], claiming that the time constants of electrochemical phenomena in fuel cells are in the order of magnitude of 10^{-19} s (Guzzella himself claimed 10^{-9} s). Pukrushpan did therefore not elaborate further on the electrochemical transient, whereas other authors have found that the time constants for the electrochemical transients are actually much higher [4,5,11,12].

Johansen investigated, in his MSc thesis [13], the possibility of using reactant feed rate as an input in a control loop. As shown in Fig. 1, when the feed rate[1] was shut down, the fuel cell continued to produce power at an almost undisturbed rate, but dropped later, after about half a minute. On the other hand, as soon as the reactant feed was reopened, the power output immediately reattained the previous values. This indicates that there is a dead time in which reactants in the manifolds must be consumed before the effect of reduced partial pressure can be appar-

[1] Johansen modified the hydrogen feed rate, but his conclusion is specular for oxygen on the cathodic side.

ent; the actual extent of this delay will depend, among other things, on the sizing of the manifolds and on the rate of consumption of reactants. This effect, which is the same one encountered at the mass-transport limit when operating a fuel cell in normal conditions, is known to be non-linear with reactant concentration, and its occurrence roughly corresponds with the depletion of one of the reactants. It must also be remarked that these effects are often not known precisely, as the cell's behaviour depends on many variables such as temperature, humidification, wear, and others.

Johansen's findings indicate that the feed rate of reactants, in the specific case of the two patents [7,8] oxygen, is a poor manipulated variable for a control layout. While it can be possible to control a fuel cell in such a way, the large delays and strong non-linearities associated with the effect of the input on the system will eventually limit the system's performance in reference tracking and disturbance rejection. Furthermore, such a system would be an energetically inefficient control through reactant starvation.

Golbert and Lewin [14] studied the application of model-predictive control (MPC) to fuel cells. They claimed that a sign inversion in the static gain between power output and current barred the possibility of using a fixed-gain controller with integral action, since it could not have been stabilised on such a process. They proceeded therefore to synthesise an MPC controller. Throughout the paper, Golbert and Lewin assume that current is a manipulable input, and use it to control the power output. However, Jay Benziger pointed out that it is not possible to use current (or voltage, which Golbert and Lewin's model also allows) as an input: he suggested the resistance of the external circuit as the variable one should rather use [15].

One of the currently few articles about fuel cells in the Journal of Process Control was written by Caux et al. [16]. They considered a system comprising a fuel cell, a compressor, valves, two DC/DC converters (a booster and a buck-boost converter). The analysis of the complete system is a step forward from the studies where the fuel cell had been seen as a separate entity from the rest of the process, but the fuel cell model itself is the same as from Amphlett et al. [3], and is therefore not treating overvoltage as a state; voltage variations will therefore be caused, directly, only by variations in temperature, current or oxygen concentration.

3. The dynamic model

In order to control fuel cells, it is useful to first present a dynamic model, in order to better understand the system. A model has been developed previously by the authors and others [12], based in particular on the work of Ceraolo et al. [4], adapted to a PBI fuel cells. PBI fuel cells are a type of fuel cells working typically between 125 and 200 °C (see for example He et al. [17] for further details), which do not rely on liquid water for membrane conductivity. The model implements the results of Liu et al. [18], includes crossover current, simplifies some assumptions on mass transport and enables the possibility of using a variable load. The main parts of the model will be shortly summarised in this section.

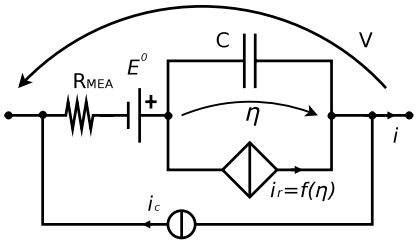

Fig. 2. A simplified model of a fuel cell, with only one electrode.

Table 1
Summary of the main equations used in the model

Cell voltage	$V = E^0 - \eta - R_{\mathrm{MEA}}(i + i_c)$	(1)
Overvoltage differential equation	$\frac{\mathrm{d}\eta}{\mathrm{d}t} = \frac{i + i_c - i_r}{C}$	(2)
Butler–Volmer equation	$i_r = i_r(\eta, \ldots)$	(3)
External load's characteristic	$f(i, V, t) = 0$	(4)

Fig. 2 shows how we can model a fuel cell to simulate its dynamic properties related to the electrochemical transient; the main equations are given in Table 1. This type of model is quite commonplace in electrochemistry, consisting of

- a voltage generator, E^0;
- a resistance, R_{MEA};
- a single electrode (the cathode), with a capacitance C in parallel with a voltage-controlled current generator;
- a current generator, i_c, that forces a certain current through the cell, even when this is in an open-circuit configuration.

It must be kept in mind that the underlying hypothesis of this simplified model, i.e. neglecting the anode, will be invalid if the hydrogen flow will be contaminated with poisons such as CO; in such a case, both electrodes will have to be modelled.

The voltage generator E^0 represents the reversible potential: it depends on temperature and concentration of reactants at the reaction sites, which in turn depends on the reaction current i_r that corresponds to the consumption of reactants. This dependence on reactant concentrations is however weak, except when some of these are close to zero. It can be calculated with thermodynamic data, and is often assumed constant at about 1.22 V.

The resistance in series with the generator, R_{MEA}, represents the resistance to proton conduction in the membrane, and any other resistances in series with it; its value depends mostly on temperature. Benziger et al. [19] claimed that R_{MEA}, in conditions of low humidification, can suddenly change its value, and that a fuel cell can exhibit ignition phenomena; these phenomena were explained by membrane

swelling with water absorption, which should not be very important in a PBI fuel cell. In Nafion-based membranes, swelling requires accumulation of water, which is determined by i_r: therefore these variations in R_{MEA} are not expected to happen when i_r and other states of the model are constant. However, hysteresis phenomena over polarisation curves taken over a time range in the order of 10^3 s have indeed been observed in PBI fuel cells, and they might be explained by mathematically similar processes, but ignition has not yet been highlighted [12].

The capacitance C lumps together a series of phenomena, most importantly the charge double layer [5] but possibly some other ones, such as charged adsorbed species. It is assumed constant, but some sources indicate it might be somewhat variable [20].

The voltage-controlled current generator $i_r(\eta)$ in parallel with the capacitance is represented, in much of the electrochemical literature, by a resistance. This can be misleading: this generator actually represents the Butler–Volmer [21] Eq. (3), that depends exponentially, not linearly, on the overvoltage η, and can depend strongly on many other factors, such as temperature, reactant concentration, presence of poisoning agents, etc. This unit also accounts for the mass-transport barrier by including reactant diffusion, which determines the value of the exchange current density, which in turn is an important term in the calculation of i_r.

The current generator, i_c, represents the crossover current, that lumps together a series of losses such as permeation of hydrogen or other reactants through the membrane, electronic conductivity of the membrane or similar ones. Its value is normally small, but has a significant effect: the overvoltage, especially the cathode's, will increase rapidly at low values of current, and the presence of this small crossover current is what reduces the open-circuit voltage of the fuel cell from the theoretical value of the reversible potential. It is assumed to be constant.

4. Instantaneous characteristics

4.1. Definition

In electrochemistry, the relationship between current density i and voltage V in a fuel cell is widely known as the polarisation curve. Polarisation curves represent the steady-state, and do not contain information about the way the fuel cell will behave during transients. To include this information in the same plot, we define the *instantaneous characteristic* to be the locus of all points that can be reached instantaneously by the fuel cell in the V–i plane. To define it, it is important to note which terms of the polarisation curve are going to change in a transient, and how so.

The instantaneous characteristic comes from Eq. (1), where the terms V and i can change stepwise. The *state* of a system is defined as the set of variables needed to fully describe a dynamic system at a given time. In the case of the model in Fig. 2 and Table 1, the voltage η across the capacitor is a state, since it represents the charge accumulated in it, which evolves continuously in time according to Eq. (2). The reaction current i_r, which represents the consumption of reactants, is a continuous, strictly increasing function of η, according to the Butler–Volmer equation [21]: i_r is therefore continuous in time as η is. To any value of η corresponds one and one only value of i_r, so the state of the fuel cell may be described by i_r just as well as by η; it is possible to express each one as a function of the other.[2] The reversible voltage E^0 will also not have a discontinuity at step time, since it weakly depends on i_r.

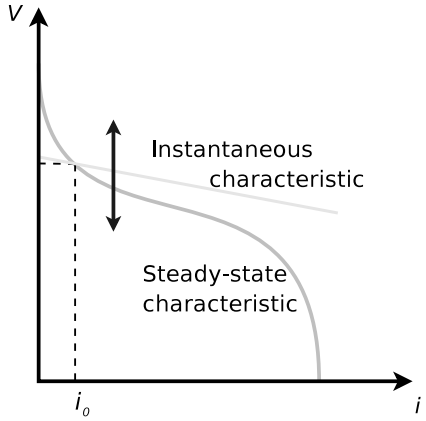

Fig. 3. The steady-state polarisation curve and the instantaneous characteristic on a V–i plane. The instantaneous characteristic can move up or down according to the value of overvoltage η.

On the other hand, the current density i passing through the fuel cell is not a state, and it can change stepwise.

The equation for the cell voltage can be rewritten highlighting the dynamic and the algebraic parts as

$$V(t,i) = \underbrace{E^0 - \eta}_{V_{\mathrm{dyn}}(t)} \underbrace{-R_{\mathrm{MEA}} \cdot (i + i_c)}_{V_{\mathrm{alg}}(i)} \tag{5}$$

If we make a stepwise change in i at $t = 0$, V_{dyn} will remain continuous, and it will have a single value at that time. V_{alg} will instead change instantaneously with i.

The instantaneous characteristic described by Eq. (5) can be seen as a line in the V–i plane that will rise or descend according to the value of $V_{\mathrm{dyn}}(t)$. It will be a straight line if R_{MEA} is constant, as shown in Fig. 3.

4.2. Application

We can now turn our attention to how specific transients develop. The values of voltage and current will be determined by the intersection between the instantaneous characteristic of the cell and the characteristic of the load. If the

[2] On the other hand, the Butler–Volmer equation, expressing $i_r = f(\eta)$, cannot be solved explicitly for η, and requires an iterative loop. The Tafel equations are a very good approximation of $\eta = f(i_r)$ at sufficiently large values of i_r [22].

intersection point is not on the steady-state polarisation curve, the cell's instantaneous characteristic will rise or sink, until the operating point will be brought to the intersection between the load characteristic and the polarisation curve.

In general, the load might also be represented by a dynamic characteristic, but for ease of treatment we will first consider only loads with a constant characteristic.

In Figs. 4 and 5, a few simple transients have been sketched. They all start from a steady-state point on the polarisation curve, and illustrate the path of the operating point to reach the new intersection between the load. All transients consist of two parts:

(1) After the step has taken place, the operating point instantaneously moves to the intersection of the current instantaneous characteristic and the new load.
(2) Remaining on the external load's characteristic, the operating point follows the movement of the instantaneous characteristic, until it settles on the intersection between the external load and the polarisation curve.

Whereas the plots in Fig. 4 assume the presence of a current or voltage generator, and therefore an external power supply, the ones in Fig. 5 assume loads that can be changed with little or no external power supply (either a variable resistance or a MOSFET). A resistance step may be done

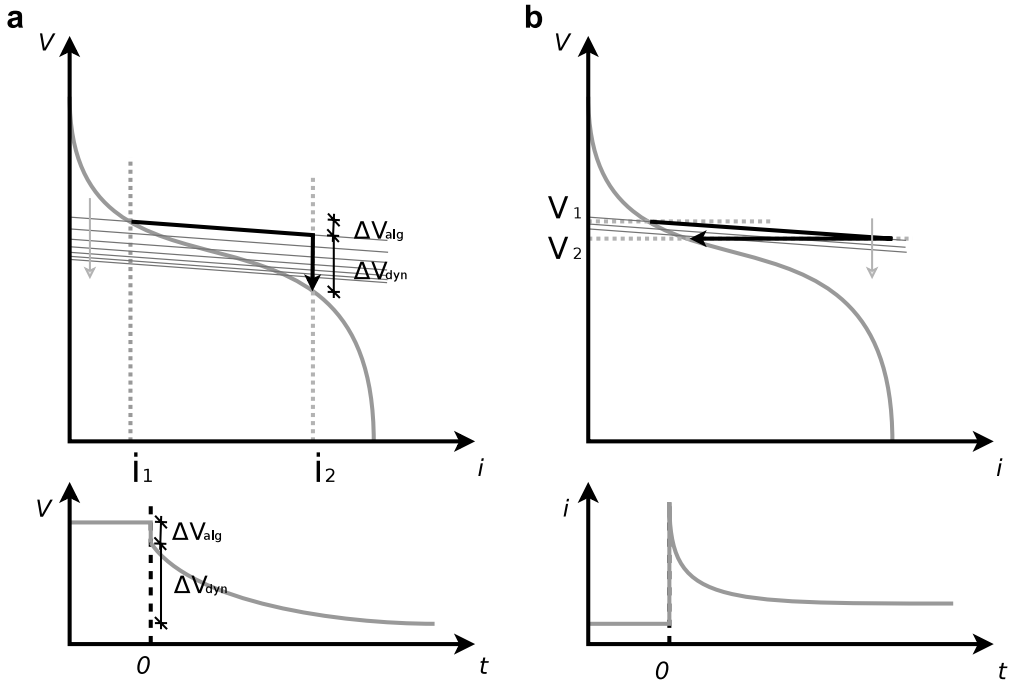

Fig. 4. Transients in the phase plane and in time when stepping (a) the cell current or (b) the cell voltage using a galvanostat or a potentiostat, respectively.

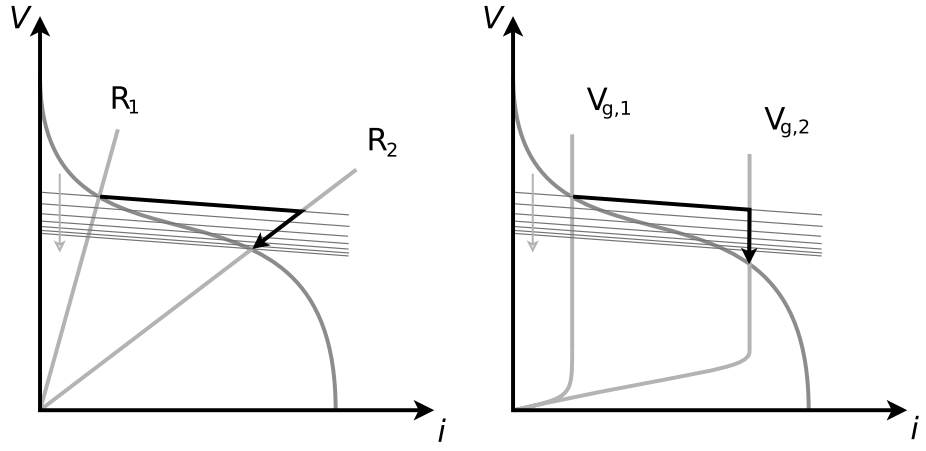

Fig. 5. Transients in the phase plane obtained by changing the external circuit's characteristic, on the left with a resistance (stepping from R_1 to R_2) connected to the fuel cell, and on the right with, in the place of the resistance, a MOSFET whose gate voltage is stepped from $V_{g,1}$ to $V_{g,2}$. The variable-resistance transient was experimentally measured by our group in laboratory experiments [12].

with a simple switch or using a rheostat; a step in the gate voltage of a MOSFET[3] will require a voltage source, but this source will have to provide only a negligible amount of power. What is particularly interesting about rheostats or MOSFETs is that they can change their characteristic continuously with an input variable that can be directly manipulated.

4.3. Time constants of the electrochemical transient

The catalytic overvoltage varies according to the differential equation

$$\frac{\mathrm{d}\eta}{\mathrm{d}t} = \frac{i + i_c - i_r}{C} = \frac{i - (i_r - i_c)}{C} \tag{6}$$

Since the level of the instantaneous characteristic is determined by the value of η, the right-hand side in Eq. (6) represents also the "speed" at which the instantaneous characteristics moves vertically on the plot. It is relatively easy to find i and $i_r - i_c$ graphically: the circuit current, i, is at the intersection of the instantaneous characteristic with the external load; the reaction current minus the cross-over current, $i_r - i_c$, is at the intersection of the instantaneous characteristic with the polarisation curve.

This claim can be demonstrated as follows: the polarisation curve represents the steady-state points, and the instantaneous-characteristic represents all points with the same η and i_r: their intersection is the steady-state with the same reaction current i_r of the transient operating point. Since at steady-state, by Eq. (2), $i_r - i_c = i$, the projection of this intersection on the i axis is $i_r - i_c$, as illustrated in Fig. 6.

An interesting side effect is that some transients may have different time constants depending on how close to the polarisation curve their trajectory is. If a transient trajectory consists of points that are close to the polarisation curve,[4] the driving force of Eq. (6), i.e. the difference between i and $i_r - i_c$, is small, and the transient will be slower. This has been verified experimentally [12], and simulation indicates that times in the order of 10 s are common to reach steady-state in open circuit. Settling times are typically in the range of 10 down to 0.1 s.

5. Perfect control of fuel cells

An important result can be obtained observing the instantaneous characteristics in the previous figures. We see clearly that they pass by the current corresponding to the maximum power output with an higher voltage than the polarisation curve, as exemplified in Fig. 7. It is an

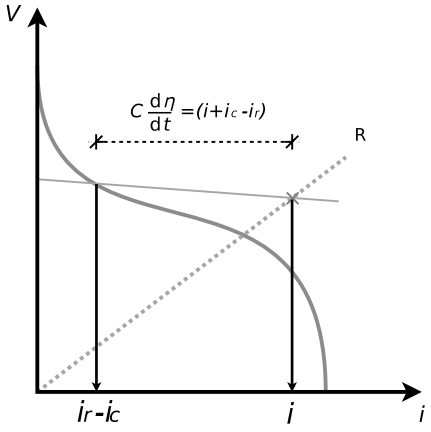

Fig. 6. The distance between the intersection points of the instantaneous characteristic with the external load and with the polarisation curve represents the driving force of the transient.

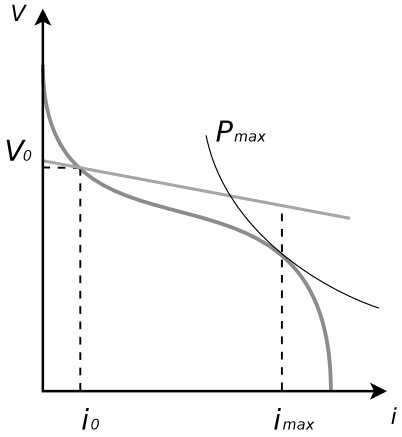

Fig. 7. At current $i_{\max}$, where the steady-state power output is maximum, the instantaneous characteristic from point (i_0, V_0) has a higher voltage than the polarisation curve.

immediate observation that this means that we can, at least in theory, step the power output of the fuel cell even beyond the maximum nominal value. We shall now seek to properly formalise this finding.

We shall define $P_{\max}$ and $i_{\max}$ to be the power output and the current at the point, on the steady-state polarisation curve, where the power output from the cell is maximum.

Theorem 5.1 (Perfect control of fuel cells). *Given a fuel cell having its steady-state voltage expressed by* $V(i) = E^0 - \eta(i_r) - R_{MEA}(i)(i + i_c)$, *with overvoltage* $\eta(i_r)$ *strictly increasing with* i_r, *and internal resistance* $R_{MEA}(i)$ *continuous in* i, *it is always possible to instantaneously step the power output to any value between zero and its maximum steady-state value from any operating point, both transient and steady-state, lying on an instantaneous characteristic intersecting the polarisation curve at some* $i \in [0, i_{\max}]$.

Proof. Given any fixed $i_0 \in [0, i_{\max}]$, we can identify the corresponding instantaneous characteristic $V(i) = E^0 - \eta(i_0 +$

[3] For a process engineer, MOSFETs can be thought as valves that allow more current through them when their gate voltage is increased. For a detailed treatise of MOSFETs, see e.g. Mohan et al. [23].

[4] More rigorously: points lying on an instantaneous characteristic whose intersection with the polarisation curve is close, with distance being measured along the i axis.

$i_c) - R_{MEA}(i)(i + i_c)$. Since $\eta(i_r)$ is strictly increasing with i_r, $\eta(i_{max} + i_c) \geqslant \eta(i_0 + i_c)$.

Subtracting the steady-state characteristic from the instantaneous one at $i = i_{max}$, we obtain $-\eta(i_0 + i_c) + \eta(i_{max} + i_c) \geqslant 0$, meaning that the instantaneous characteristic will have a higher voltage at $i = i_{max}$, and thereby a larger power output.

Power along the instantaneous characteristic varies continuously, according to the formula $P(i) = V(i)i$, because $R_{MEA}(i)$ is also assumed continuous. It is trivial that power output can be set to zero by setting $i = 0$. For the intermediate-value property, $\exists i{:}P(i) = P, \quad \forall P \in [0, P_{max}]$. □

This theorem guarantees, therefore, that there is a way to change instantaneously to any value of power output in the complete power range of the fuel cell, from zero to maximum, under very general conditions. This means there is no inherent limitation to how fast control we can achieve, even though practical issues such as measurement time and computation time will eventually pose a limit.

This has also other implications: if incorrectly controlled, a fuel cell might exhibit large spikes in power output, which may damage equipment connected to it. This might be especially important in microelectronics appliances.

5.1. Implicit limitations

Theorem 5.1 delivers an important result, but makes some implicit assumptions. The assumption about the form of the function describing the polarisation curve is especially important, since the curve is expected to be only a function of the circuit and reaction currents: other factors such as temperature, catalyst poisoning, reactant concentration are left out. In particular, increased water content in the membrane and increased temperature due to heat dissipation may reduce resistance at higher currents, after their respective transients settle: this would make R_{MEA} dependent on time, which invalidates one of the theorem's hypotheses.

Therefore, *the theorem is valid only in the context of a certain set of states* that define the polarisation curve: we are only guaranteed that we can instantly reach the maximum power output for those conditions of temperature, composition, water content and other variables describing the state of the fuel cell stack, which may be less than the nominal power output that the fuel cell is supposed to deliver in design conditions. In such a case, other control variables may be used to modify these states, and might pose some performance limits; for instance, a temperature increase in the cell cannot occur stepwise.

This paper is mainly concerned about the control of power output from the fuel cell, and assumes that reactant and temperature control is ensured by another control system; see for example Pukrushpan [9] for a detailed analysis of reactant control for cathode and anode. The dynamic responses of these control loops are slower than the electrochemical transient, but, as long as the reactant concentration is sufficient to sustain the required current and power output, perfect control will still be possible (albeit with larger losses than at steady-state). In other words, there is a lower, variable tolerance limit for reactant concentration that must be ensured by the flow control system.

6. Fuel cells and DC/DC converters

Having shown with Theorem 5.1 that the electrochemistry in fuel cells poses no inherent limitation to how fast the power output can be changed, we can now look at how this power output may be managed in order to be consistent with an application's requirements.

One possibility is using linear control, intended as placing a variable load, such as a rheostat or a MOSFET, in the circuit ("line") between the fuel cell and the load. The resistance of this new component can then be manipulated to control some system parameters, such as the voltage applied on the load or the circuit current. Whereas this layout is simple, it is also inherently inefficient, as the manipulated load is effectively dissipating excess power, and it is also unable to provide the load with voltages beyond the fuel cell's.

In order to have a more efficient conversion of power from the fuel cell stack to the load, we will consider the application of DC/DC converters.

A DC/DC converter has the objective of transforming the power from the fuel cell in an appropriate form. According to Luo and Ye [24], there are over 500 different topologies of converters. The most simple are the *boost* converter, that increases voltage from input to output, and the *buck* converter, that decreases it; other types are the *buck-boost* and the *Ćuk* converters.

The buck-boost converter is chosen for this paper. The reasons are that it can convert power in a wide range of voltages, both above and below the cell stack's: the buck or the boost converters alone, instead, could only respectively reduce or increase the input voltage. The buck-boost converter is also simpler than the Ćuk converter, having only two states instead of four.

In a real application, a more complex layout may be preferred, to include the possibility of regenerative braking and reverse drive. For sake of simplicity, this study will consider only the case of a simple converter.

In this paper, the control objective for the DC/DC converter will be to control its output voltage in spite of external disturbances, rather than its power throughput: this is motivated by the common usage of voltages as input variables in DC motors. The control performance will be limited by the duty-cycle period: shorter periods will improve performance, but will also increase the losses in the switching elements; the precise value chosen for the duty-cycle period will depend on the physical characteristics of the converter and on design decisions. In this paper we assumed values in the range of 10–100 μs.

6.1. Fuel cells coupled with converters

In buck-boost converters, we usually have a discontinuous current passing through the input, in our case a fuel cell stack. Since the switching frequency will in most cases be much faster than the transients in the cell, it is common to work with averaged units [25].

Of particular interest is the case of a current stepping between a certain value and zero at regular intervals. Defining D to be the fraction of time during which a current I passes through the cell, we find that the reaction current (the one corresponding to the consumption of reactants) is $I_r = ID$ when averaged over a sufficiently long time.[5] If the switching frequency is substantially faster than the electrochemical dynamics, we may assume the overvoltage to be constant: $\eta \approx \eta(iD)$. However, the cell voltage loss caused by the linear resistance has no transient associated, and will depend directly on the current, no matter it is applied only a fraction of the time. Therefore, calling V_W, or *working voltage*, the voltage obtained by a fuel cell under a rapidly switching current that has value I for a fraction D of the time, we obtain:

$$V_W = E - \eta(iD) - RI \tag{7}$$

This voltage is the actual input voltage that the DC/DC converter will work with.

6.2. Buck-boost converters

A buck-boost converter is sketched in Fig. 8. The voltage source is connected in parallel, through a switch, to an inductor. When the switch is on, the inductor accumulates power by storing energy in its magnetic field.

The inductor current varies continuously, as it is a state. When the switch is off, the current is therefore forced into the capacitor that the inductor is now in parallel with, moving the energy stored in the inductor's magnetic field into the capacitor's electric field.

Independently from the switch's state, the capacitor is continuously exchanging power with an external load.

In this layout, we assume that the cell stack's voltage V_W and the external load's current I_a are measurable at all times.

Since we know from Theorem 5.1 that fuel cells can immediately deliver their maximum power, the DC/DC converter will set the performance limit. Lower values for the capacitance and the inductance will increase the transient's speed and accelerate the overall response, but will require faster switching. In this paper we will use the values previously used in a boost converter designed in Caux et al. [16], namely $L = 0.94$ mH and $C = 3.2$ mF.

The equations describing this system are, when the fuel cell stack is connected to the inductor (the ON position in Fig. 8)

[5] Here we are neglecting the effect of the crossover current for ease of notation.

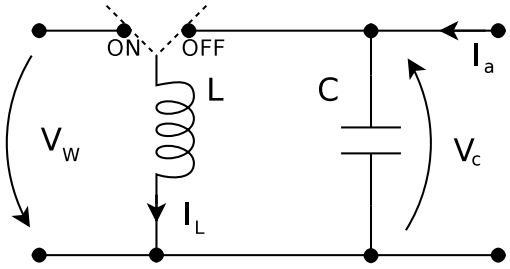

Fig. 8. A basic representation of a buck-boost DC/DC converter; V_W is the input voltage.

$$L\frac{dI_L}{dt} = V_W \tag{8}$$

$$C\frac{dV_C}{dt} = -I_a \tag{9}$$

V_W and I_a are considered to be external entities with respect to the converter, and are assumed to maintain a positive sign. The trajectories described by these equations are straight lines, since I_a and V_W are assumed not to depend directly on I_L or V_C.[6]

When the switch is positioned so that the inductor is connected to the capacitor (the OFF position in Fig. 8), the equations are instead

$$L\frac{dI_L}{dt} = -V_C \tag{10}$$

$$C\frac{dV_C}{dt} = I_L - I_a \tag{11}$$

The trajectories described by these equations are a series of ellipses, centred at the point $(0, I_a)$, whose parametric equation can be given as

$$\frac{1}{2}L(I_L - I_a)^2 + \frac{1}{2}CV_C^2 = k \quad k \in \mathbb{R}_0^+ \tag{12}$$

Obviously, if I_a were to change, the centre of the ellipses would move and the actual trajectory of a point could not resemble an ellipse at all.

It would be tempting to define these curves as representatives of the amount of energy physically stored in the converter, but the first term in Eq. (12) is not the energy stored in the inductor's magnetic field. The value of k, however, can indeed be mathematically interpreted as representative of the system's energy.

The trajectories corresponding to these equations are shown in Fig. 9. The ON mode is represented on the left-hand side, where energy is collected from the input by the inductor. On the right-hand side (the OFF mode), no energy is drawn from the source, and the energy stored in the inductor is exchanged with the capacitor. The capacitor exchanges power with the output in both configurations. In

[6] In reality, V_W depends on I_L, as $V_W = E - \eta - R\,I_L$. However, such an assumption would require a cell-specific parameter, R, to be provided. It will be assumed that R is small enough to justify an assumption of positive V_W in the area of interest.

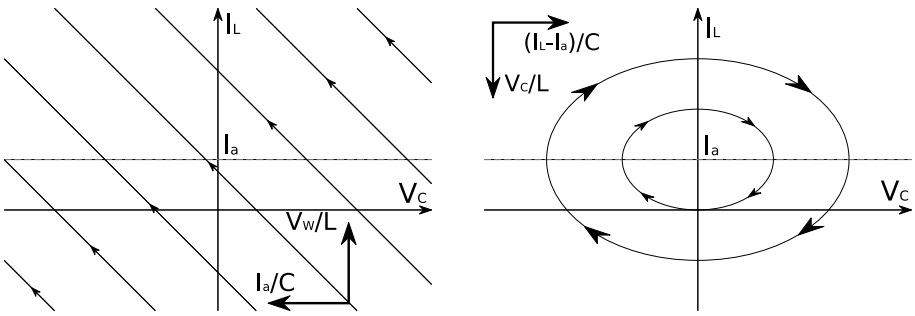

Fig. 9. The trajectories of the state variables in a buck-boost converter in the V_C–I_L plane for given values of external disturbances V_W, I_a.

a real system, the trajectories in the right-hand sides would be spirals, because of losses in the switches.

6.3. Control of DC/DC converters

The control problem for a DC/DC converter is to set the converter's output voltage, V_C, by properly manipulating the converter's switch, in spite of disturbances V_W, which depends on the cell stack, and I_a, which depends on the load. Converter control is not a trivial issue: one problem is that both positions of the converter switch result in no power being transferred from the fuel cell at steady-state.

The most common techniques to control a converter are pulse-width modulation [26] and sliding-mode control [27]. In pulse-width modulation, a *duty ratio D*, representing the fraction of time the switch is in the ON position, is varied between 0 and 1. In sliding-mode control, instead, the switch is set to ON or OFF state depending on a set of logic rules, which are recalculated at very short intervals. Another possible technique is model-predictive control, as suggested by Geyer et al. [28]; since the time required for online optimisation largely exceeds the requirements, the authors suggested using a state-feedback piecewise affine controller [29]. Application of $\mathscr{H}_\infty$ controllers has also been studied [30].

This paper will adopt an approach similar to sliding-mode control by defining some *switching rules*. Instead of the usual constant sliding surfaces as described by Spiazzi and Mattavelli [27], a series of variable surfaces were devised to take advantage of the shape of trajectories of the system in the V_C–I_L plane. This is helpful as their shape can change considerably depending on external disturbances (such as I_a and V_W), which represent the effect of having a variable voltage source and an unknown load. This is strictly speaking not sliding-mode control, as no one of the defined surfaces will actually be a sliding mode. The rules, however, do make sure that the desired output is attained.

Since the load to which the converter will deliver the power has not yet been defined, the load current I_a will be considered as a disturbance that the converter will have to be able to compensate for; it is however possible that the external control loop, which will use the DC/DC converter as an actuator, will have to control I_a by varying the converter's output, V_C.

6.4. Control rules

Control of the converter will be understood having the following objective: to control the output voltage V_C so that it is close to reference V_{ref}, in spite of external disturbances I_a and V_W, by manipulating the switch in the buck-boost controller. In other words, we will try to maintain a certain value of the converter's output voltage by switching the system between its two substructures (as shown in Figs. 8 and 9), accounting for the changes in output current (caused by the load) and input voltage (caused by the fuel cell stack). The rules will have to be calculated at each iteration, using new measurements for V_W, I_L, V_C and I_a, and are formulated as follows:

6.4.1. Energy level

If the value of k in Eq. (12) is not sufficiently high, the elliptical trajectories of the OFF mode will not be able to reach V_{ref}. Therefore, the only possibility left is to switch to the linear trajectories of the ON mode until a sufficiently high energy level is reached.

The *sufficiently high* energy level is however not the one corresponding to an ellipse that has its extreme point in V_{ref}. If it were so, it would not be possible to maintain the operating point at that value by switching to the ON mode: the ON mode, which in general has a non-zero component along the V_C axis, would cause the system to go towards a lower energy level, at which it should maintain the ON state until reaching again a high enough energy level. An hysteresis cycle would then result, which would be an unsatisfactory performance.

The correct energy level is then the one corresponding to the ellipse that, at the reference voltage V_{ref}, is *tangent* to the lines of the ON mode. The unavoidable imprecision in parameter estimation and measurement will cause some oscillation, however.

The mathematical description of the rule is

$$\frac{1}{2}CV_C^2+\frac{1}{2}L(I_L-I_a)^2<\frac{1}{2}CV_{ref}^2+\frac{1}{2}L\left(\frac{V_{ref}I_a}{V_W}\right)^2 \Rightarrow \text{ON} \tag{13}$$

6.4.2. High-voltage switch

At voltages higher that V_{ref}, the surface at which one moves from one substructure to the other is given by the tangent line departing from the ellipse described above, at voltage V_{ref}. Since this line is by construction parallel to the lines of the ON mode, once the operating points, moving along the OFF-mode ellipses, crosses this line, it is not possible for it to return back. This is important because there is no guarantee that the component of the ON-mode derivatives along a given line are larger than the OFF-mode's, because the former are disturbances that we do not directly control.

The mathematical description of the rule is:

$$V_{\text{C}} > V_{\text{ref}} \wedge I_{\text{L}} - I_{\text{a}} < \frac{V_{\text{ref}} I_{\text{a}}}{V_{\text{W}}} - \frac{C}{L}\frac{V_{\text{W}}}{I_{\text{a}}}(V_{\text{C}} - V_{\text{ref}}) \Rightarrow \text{ON} \tag{14}$$

6.4.3. Low-voltage switch

It is not unlikely that, during transients, voltage V_{C} will reach negative values. In fact, it is quite a common phenomenon, albeit lasting only for a short time. A reasonable control objective is to minimise the inverse response during such a transient. Therefore, if during a transient V_{C} is less than zero, and the energy level is sufficient as defined above, the switch from ON mode to OFF mode should be at the point where the ON lines are tangent to an ellipse, which is at the lowest energy level they will reach.

The mathematical description of the rule is:

$$V_{\text{C}} < 0 \wedge I_{\text{L}} - I_{\text{a}} < \frac{V_{\text{C}} I_{\text{a}}}{V_{\text{W}}} \Rightarrow \text{ON} \tag{15}$$

6.4.4. No negative currents

An additional rule may be easily implemented if we desired to avoid negative values of current I_{L}, but the short duration of transients should not pose a threat of reverse electrolysis.[7] However, if that were the case, one could simply implement:

$$I_{\text{L}} < 0 \Rightarrow \text{ON} \tag{16}$$

6.4.5. Combining the rules

The first three rules (not the rule against negative current) are graphically plotted in Fig. 10. If no rule should match, the default state of the switch will be OFF.

6.5. Performance of the switching rules

Some preliminary conclusions can be drawn by looking carefully at Fig. 10.

[7] Of course this is relevant only for the ON mode, when current is actually passing through the fuel cell stack.

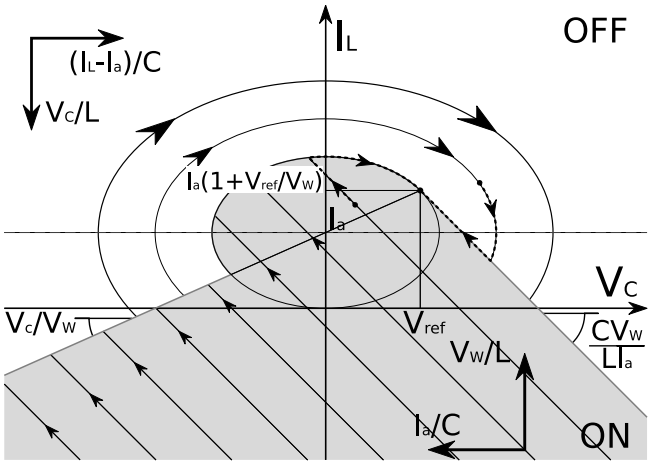

Fig. 10. Graphical representation of the switching rules to control a buck-boost converter. Notice that the inclination of the ON lines (in the greyed-out area), the inclination of the switching lines at high and low voltage, and the size and vertical positioning of the central elliptical part all depend on the values of the reference voltage and the disturbances. Two possible trajectories, from higher and lower values of V_{C} to reach V_{ref}, are sketched.

- Steps in V_{ref} will in general exhibit an inverse response. When increasing, the operating point will have to accumulate energy along the ON-mode lines, which will cause an initial reduction of V_{C}. When decreasing, the operating point will follow the OFF-mode lines until it will reach either their maximum value of voltage, or the switching surface described by rule Eq. (14) before decreasing again.
- Steps in I_{a} will have a similar effect, but this is intuitive: more current at the output, at the same output voltage, means more power delivered, and the converter will have to gradually adapt to this new regime.
- The set of rules does not permit to specify a negative V_{ref}. This is intentional, because, with a positive I_{a}, power would be drawn from the outer circuit to the fuel cell, causing reverse electrolysis, and likely damaging the fuel cell's catalyst.

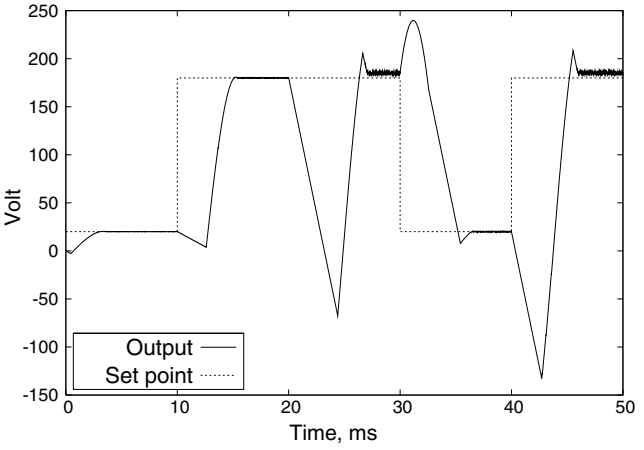

Fig. 11. Simulated transient of a buck-boost converter, controlled with switching rules. The external current is initially 20 A, and is stepped to 180 A after 20 ms. The switching frequency has been set to 10 μs.

A simulated transient is shown in Fig. 11. It can be noticed how the inverse response is much more significant at high values of I_a. The transients have typically quick settling times, about 5 ms: this is faster than the 0.2 s required for vehicles (according to Soroush [31]), and can make this control strategy useful also for microelectronic applications such as laptops and mobile phones.

The steady-state error that is present in two of the high-voltage regimes shown in Fig. 11 is due to modelling error. At high values of I_a and V_C, the dependence of V_W on I_L becomes sufficiently large to prevent convergence. However, the error is small, and, when using this control method in an internal loop of a cascade control layout, the external feedback loop will compensate for this.

6.6. Computational efficiency

The simulation times with the switching-rule controller are relatively long; the transient in Fig. 11 requires about 50 s to calculate on a 2-GHz, 32-bit desktop computer running Simulink. This makes simulation over longer time spans unpractical. The fuel cell's overvoltage, when starting the simulation, needs some time to reach a steady-state value from zero, and this initialisation transient may interfere with the transients we are interested in measuring.

The main reason for such an unsatisfactory computational efficiency is that the rules are evaluated every 10 μs, and a transient has to be calculated every time the algorithm requires a switch. When the transients settle.[8] the manipulated variable does not attain a constant value, but is continuously switched between ON and OFF.

Using another model that would allow the usage of a continuous manipulated variable and averaged values for other variables would likely improve the simulation performance, even though the control performance might be reduced because of the additional level of abstraction. Pulse-width modulation is another common technique in converter control that might provide these benefits. The option of using pulse-width modulation in this setting is currently being investigated.

7. Application to a DC electric motor

It has been shown in Figs. 4 and 5 that the shape of the characteristic of the external load has a strong effect on how the transient develops in the fuel cell. It is therefore generally desirable, when designing a controller for a fuel cell, to consider a description of the load as well. In other words, the control system is not for the fuel cell alone, but for the whole system. In this section, a simple electric motor for a fuel cell powered car will be considered; for simplicity, a regenerative braking system is not going to be modelled.

[8] In reality, only *macroscopic* transients settle, because the control algorithm is indeed based on rapidly switching between two transients compensating each other.

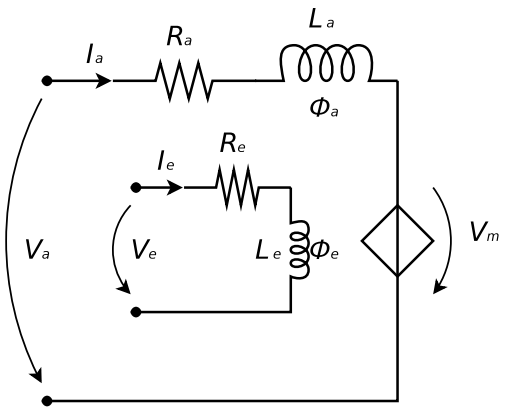

Fig. 12. A typical model of a DC motor [34].

7.1. Electric DC motors

Direct-current motors have for a long time been the only type of electric motor that could be easily controlled. The reason of this preference is due to the simplicity of controlling the main variable in DC motors, the input current, as opposed to the difficulty of controlling the input frequency in alternated-current motors. Whereas microelectronics has made it practical to control AC motors too, all electric motors can be modelled as DC motors [32]: therefore, this paper will consider a DC motor as the load to which the fuel cell is connected.

Generally speaking, there are two main variables influencing the power output in a DC motor's mathematical model (Fig. 12): the armature current and the field-winding current. The armature current, I_a, is directly proportional to the torque exerted by the motor, divided by the magnetic field Φ_e. The voltage generator V_m in Fig. 12 represents the counter-electromotive force induced by the rotation of the shaft. Its value is directly proportional to the angular velocity multiplied by the magnetic flux Φ_e.

The field-winding current, which usually absorbs just a small fraction of the total power consumption, generates the magnetic field in which the armature current passes; by weakening the field, it is possible to increase velocity at the expense of torque, by modifying the proportionality ratio between armature current and torque [34].

Such a simplified model can be described by the following equations:

$$V_a = R_a I_a + L_a \frac{dI_a}{dt} + V_m \tag{17}$$

$$V_m \propto \omega \Phi_e \tag{18}$$

$$I_a \propto \frac{T}{\Phi_e} \tag{19}$$

7.1.1. Control variables

Rearranging Eq. (17), we can more easily see that I_a is a state[9] of the motor.

[9] *State* means here a variable that is a differential state in an ordinary differential equation.

$$L_a \frac{dI_a}{dt} = V_a - R_a I_a - V_m \tag{20}$$

From here, it is easy to transpose this equation in the Laplace domain

$$I_a = \frac{1}{L_a s + R_a}(V_a - V_m) \tag{21}$$

Typical values of 20 mH for L_a and 20 mΩ for R_a will be used. For more data, refer to Larminie and Lowry [33], Leonhard [34], or Ong [35].

A graphical representation of this system is presented in Fig. 13. We see clearly that I_a is the output and $V_a - V_m$ is the input. The problem of controlling an electric motor often involves the control the armature current [36], and we therefore assume I_a to be our controlled variable.

The counter-electromotive force V_m is a consequence of vehicle motion, which is often determined by an external control loop (such as a driver acting on the accelerator and brake pedals). V_m will therefore be interpreted as a disturbance on the process input. It is possible to compensate for this disturbance by manipulating the input voltage V_a. The control problem is therefore to control I_a by manipulating V_a, in spite of disturbance V_m.

We can set voltage V_a by connecting the motor input to a buck-boost converter's output. The control performance that was indicated in the section on converter control can be now interpreted as actuator dynamics. This is an example of cascade control: control of I_a is obtained by controlling V_C, which is in turn obtained by switching between the buck-boost converter's ON and OFF modes.

7.2. PI controller synthesis

In order to obtain a controller $K(s)$ as in Fig. 14, it can be useful to approximate the actuator dynamics as a transfer function. Looking at Fig. 11, we can assume that the actuator dynamics can be approximated by the following transfer function:

$$A(s) = \frac{e^{-\theta s}}{\tau s + 1} \tag{22}$$

where the delay θ is estimated at 4 ms and the time constant τ at 1.5 ms. The delay θ is assumed to be an effective delay, actually representing the inverse response; Skogestad [37] claims that "*an inverse response has a deteriorating effect on control similar to that of a time delay*".

Having an approximate linear description of the system, we can proceed to synthesise a PI controller according to the SIMC rules [37]. The resulting controller is:

$$K(s) = K_c\left(1 + \frac{1}{\tau_I s}\right) \tag{23}$$

where we have selected $K_c = 3.125$ and $\tau_I = 32$ ms.

It is now possible to make simulation runs of the whole control system. However, due to the complexity that the model has attained at this point, especially in its rapid switching rules for the DC/DC converter, it is not practical, in terms of computational time, to simulate an entire driving cycle as those issued by various authorities. On a 2-GHz, 32-bit computer, the simulations in Figs. 15 and 16 take about 90 s; on the same computer and in equal conditions, the transient with a linear $A(s)$ is calculated almost instantaneously.

As an indicator of performance, the linear approximation of Eq. (22) may be used, but it will obviously not give any information about the fuel cell during the simulation run. It is expected that using control methods based on averaged quantities, such as pulse-width modulation, will reduce the requirements to the point where simulations in the range of hours will be reasonably computationally cheap. Using the current complete model, however, one can simulate some specific transients and observe the control performance.

A brief series of transients is simulated in Figs. 15 and 16, where a series of steps in the armature current's refer-

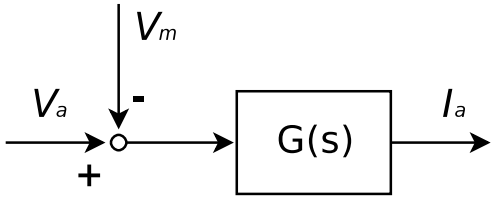

Fig. 13. The process flow diagram of a simple DC motor with constant magnetic flow; its transfer function is expressed by $G = \frac{1}{L_a s + R_a}$, as shown in Eq. (21).

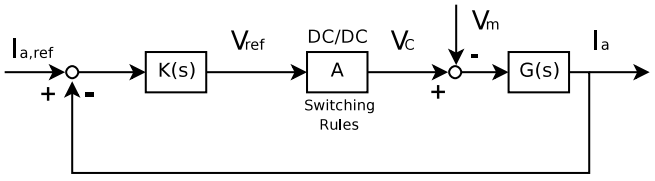

Fig. 14. The control structure of the proposed layout.

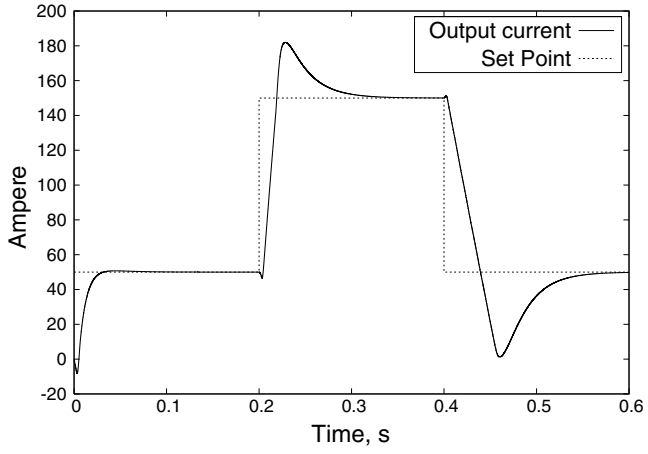

Fig. 15. Simulation of a series of steps in reference for the system in Fig. 14. The switching frequency in the converter is 100 μs.

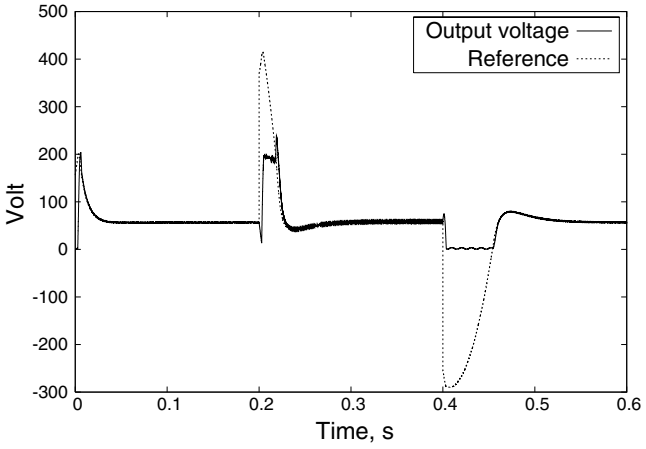

Fig. 16. The PI controller's output V_{ref} and the actual converter output V_C corresponding to the simulation in Fig. 15. The output of the controller has been limited to $V_{ref} \in [0, 200]$V.

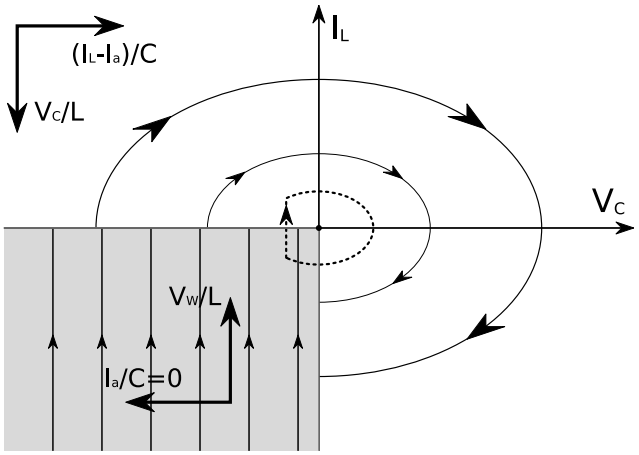

Fig. 17. The approximate trajectory of the operating point when $V_{ref} = 0$ and $I_a = 0$. Higher switching frequencies will shrink the trajectory towards the origin.

ence is performed. It is assumed that the counter-electromotive force is constant at 55.6 V, for simplicity and to make the results comparable. The values of the load current are plotted in Fig. 15, whereas the corresponding output voltage from the DC/DC converter, which is also the motor's input voltage, is plotted in Fig. 16.

The resulting control performance seems to be satisfactory, with rise times of at most 50 ms in all transients; some overshoot is observed, but the transient is settled in all cases after 0.2 s.

7.3. Limitations on controller output

In the simulation, the output of the controller has been limited to $V_{ref} \in [0, 200]$ V. Therefore, when the controller would require a value outside this interval, the exceeding amount of control action will be ignored. This can, in principle, cause problems related to wind-up; indeed, the transients presented appear to be consistently slower when their manipulated variable has been saturated for a longer time.

Whereas the upper bound on V_C is somewhat arbitrary, under no condition should it be made possible for the controller to require a negative voltage. This would mean that power is being absorbed in the fuel cell stack, and reverse electrolysis or other damaging phenomena will rapidly occur. In this configuration, the reduction of I_a is possible only through the disturbance V_m (proportional to vehicle velocity) and through resistance R_a, with a time constant of about one second. In fact, with the proposed control configuration, the control system may experience significant wind-up problems in a case as trivial as $I_{a,ref} = 0$, $V_m = 0$, that is a vehicle standing still. In a real vehicle, this would just translate to some torque in the motor being compensated by braking action.

Another issue is when the converter is required to produce exactly 0 volts, even if I_a is larger than 0. This happens anytime the PI controller requires a negative voltage. The converter's switching rules degenerate in a special case: output voltage oscillates around the origin in an asymmetrical fashion, sketched in Fig. 17, resulting in a net average positive value of V_C and possibly wind-up issues. This is visible in Fig. 16 at the beginning of the last transient. While the amplitude of such oscillations can be reduced with a higher switching frequency, their average value will always be positive.

To resolve this problem, a new simple rule for the converter will be added

$$V_{ref} \leqslant 0 \Rightarrow \text{OFF} \tag{24}$$

It is important to notice that rule 24 takes precedence on all others, since it might be contradicting them. The meaning of this rule is that the fuel cell stack must be disconnected whenever there is an unachievably low objective. In a real application, the voltage will then gradually decrease to zero because of dissipation in the motor and in the converter switches, or because of storage in a battery or supercapacitor.

The last transient of Figs. 15 and 16 with this new rule is shown in Figs. 18 and 19. There is a clear oscillatory interval where the average value of V_C is zero. The overall

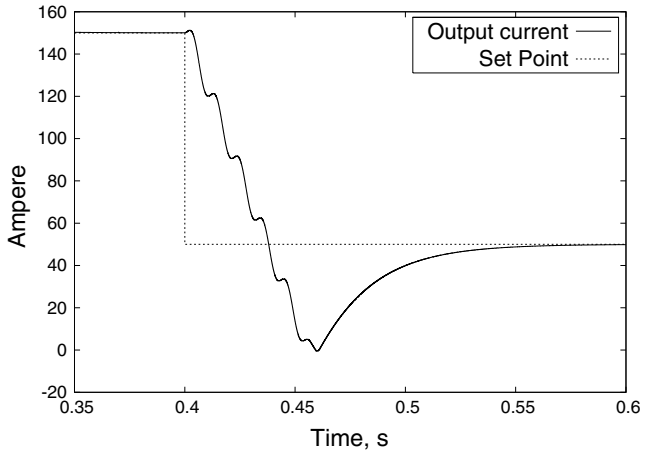

Fig. 18. Recreation of the last transient in Fig. 15 after the introduction of rule 24.

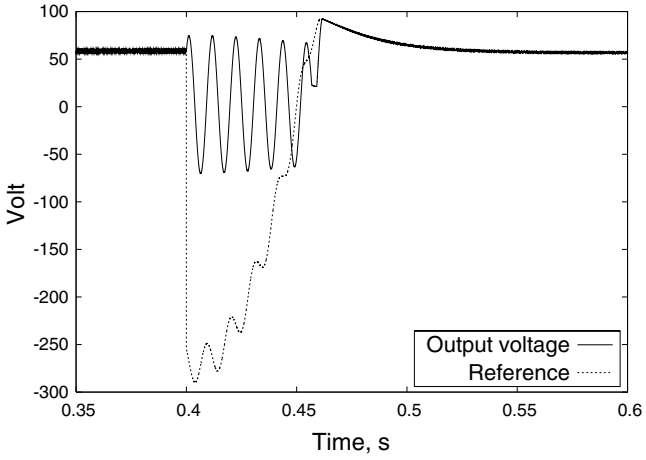

Fig. 19. Recreation of the last transient in Fig. 16 after the introduction of rule Eq. (24).

dynamics may be marginally faster, but the most important result is the disconnection of the fuel cell stack when its power is not needed.

8. Conclusion

This article has first analysed from a theoretical point of view the electrochemical transient of fuel cells, introducing the concept of instantaneous characteristic of a fuel cell and how it influences the shape of transients in the phase plane of voltage versus current density.

These results have been used to demonstrate that it is always possible to instantaneously step the power output of a fuel cell to its maximum (meant as the maximum at the present temperature, partial pressures, catalyst poisoning etc.) under broad conditions.

A method to control the output voltage of a buck-boost converter connected to a fuel cell was presented. The method is based on switching the converter based on a few simple logical rules. The resulting performance has been deemed satisfactory, with transients settling after about 5 milliseconds. The requirements on computational time for this strategy, however, make it difficult to simulate the control system over longer time spans, such as standard driving cycles; using an averaged-quantity method such as pulse-width modulation is suggested as a means to improve the computational performance.

The resulting control loop has then been inserted in a cascade-control framework (Fig. 14) to control the armature current in a DC motor by manipulating its input voltage. The results have been in excess of specifications given elsewhere in the literature [31], with rise times of about 50 milliseconds and settling times of less than 0.2 s (Fig. 15).

Acknowledgement

This work has received financial support from the Norwegian Research Council and Statoil AS.

References

[1] F. Zenith, S. Skogestad, Dynamic modelling and control of polybenzimidazole fuel cellsProceedings 18th International Conference on Efficiency, Cost, Optimization, Simulation and Environmental Impact of Energy Systems (ECOS), vol. 3, Tapir Academic Press, Trondheim, Norway, 2005, pp. 1203–1210. http://www.nt.ntnu.no/users/skoge/publications/2005/zenith_ecos2005/.

[2] J.B. Benziger, M. Barclay Satterelid, W.H. Hogarth, J.P. Nehlsen, I.G. Kevrekidis, The power performance curve for engineering analysis of fuel cells, Journal of Power Sources 155 (2006) 272–285.

[3] J.C. Amphlett, R.F. Mann, B.A. Peppley, P.R. Roberge, A. Rodrigues, A model predicting transient responses of proton exchange membrane fuel cells, Journal of Power Sources 61 (1996) 183–188.

[4] M. Ceraolo, C. Miulli, A. Pozio, Modelling static and dynamic behaviour of proton exchange membrane fuel cells on the basis of electro-chemical description, Journal of Power Sources 113 (2003) 131–144.

[5] P.R. Pathapati, X. Xue, J. Tang, A new dynamic model for predicting transient phenomena in a PEM fuel cell system, Renewable Energy 30 (2005) 1–22.

[6] H. Weydahl, Dynamic behaviour of fuel cells, PhD thesis, Norwegian University of Science and Technology, Trondheim (August 2006).

[7] H. Lorenz, K.-E. Noreikat, T. Klaiber, W. Fleck, J. Sonntag, G. Hornburg, A. Gaulhofer, Method and device for vehicle fuel cell dynamic power control, US patent 5 646 852, assigned to Daimler-Benz Aktiengesellschaft (July 1997).

[8] W.E. Mufford, D.G. Strasky, Power control system for a fuel cell powered vehicle, US patent 5 771 476, assigned to DBB Fuel Cell Engines GmbH (June 1998).

[9] J.T. Pukrushpan, Modeling and control of fuel cell systems and fuel processors, PhD thesis, Department of Mechanical Engineering, University of Michigan, Ann Arbor, Michigan, USA (2003).

[10] L. Guzzella, Control oriented modelling of fuel-cell based vehicles, in: NSF workshop on the integration of modeling and control for automotive systems, 1999.

[11] H. Weydahl, S. Møller-Holst, G. Hagen, Transient response of a proton exchange membrane fuel cell, in: Joint International Meeting of The Electrochemical Society, 2004.

[12] F. Zenith, F. Seland, O.E. Kongstein, B. Børresen, R. Tunold, S. Skogestad, Control-oriented modelling and experimental study of the transient response of a high-temperature polymer fuel cell, Journal of Power Sources 162/1 (2006) 215–227.

[13] R.L. Johansen, Fuel cells in vehicles, Master's thesis, Norwegian University of Science and Technology, 2003.

[14] J. Golbert, D.R. Lewin, Model-based control of fuel cells: (1) regulatory control, Journal of Power Sources 135 (2004) 135–151.

[15] J. Benziger, oral comment at the annual meeting of the American Institute of Chemical Engineers in Austin, 2004.

[16] S. Caux, J. Lachaize, M. Fadel, P. Shott, L. Nicod, Modelling and control of a fuel cell system and storage elements in transport applications, Journal of Process Control 15 (2005) 481–491.

[17] R. He, Q. Li, G. Xiao, N.J. Bjerrum, Proton conductivity of phosphoric acid doped polybenzimidazole and its composites with inorganic proton conductors, Journal of Membrane Science 226 (2003) 169–184.

[18] Z. Liu, J.S. Wainright, M.H. Litt, R.F. Savinell, Study of the oxygen reduction reaction (ORR) at Pt interfaced with phosphoric acid doped polybenzimidazole at elevated temperature and low relative humidity, Electrochimica Acta 51 (2006) 3914–3923.

[19] J. Benziger, E. Chia, J.F. Moxley, I. Kevrekidis, The dynamic response of PEM fuel cells to changes in load, Chemical Engineering Science 60 (2005) 1743–1759.

[20] A. Parthasarathy, B. Davé, S. Srinivasan, A.J. Appleby, C.R. Martin, The platinum microelectrode/Nafion interface: an electrochemical impedance spectroscopic analysis of oxygen reduction kinetics and

Nafion characteristics, Journal of the Electrochemical Society 139 (6) (1992) 1634–1641.
[21] C.H. Hamann, A. Hamnet, W. Vielstich, Electrochemistry, Wiley-VCH, 1998.
[22] J. Larminie, A. Dicks, Fuel Cell Systems Explained, first ed., Wiley, 1999.
[23] N. Mohan, T.M. Undeland, W.P. Robbins, Power Electronics: Converters, second ed.Applications and Design, John Wiley & Sons, Inc., 1995.
[24] F.L. Luo, H. Ye, Advanced DC/DC Converters, CRC Press, Boca Raton, Florida, USA, 2004.
[25] J.P. Agrawal, Power Electronic Systems — Theory and Design, Prentice Hall, 2001.
[26] M. Giesselmann, H. Salehfar, H.A. Toliyat, T.U. RahmanThe Power Electronics Handbook, Industrial Electronics, CRC Press, 2001, Chapter 7 – Modulation Strategies.
[27] G. Spiazzi, P. MattavelliThe Power Electronics Handbook, Industrial electronics, CRC press, 2001 (Chapter 8 – Sliding-Mode Control of Switched-Mode Power Supplies).
[28] T. Geyer, G. Papafotiou, M. Morari, On the optimal control of switch-mode DC–DC converters, Hybrid Systems: Computation and Control 2993 (2004) 342–356.
[29] M. Morari, Beyond process control, in: Proceedings of the 13th Nordic Process Control Workshop, Lyngby, Denmark, 2006.
[30] R. Naim, G. Weiss, S. Ben-Yaakov, H^{∞} control applied to boost power converters, Transactions on Power Electronics 12 (4) (1997) 677–683.
[31] M. Soroush, Y.A. Elabd, Process systems engineering challenges in fuel cell technology for automobiles, in: AIChE Annual Meeting, 2004.
[32] S.E. Gay, M. Ehsani, Impact of electric motor field-weakening on drive train oscillations, in: Electric Machines and Drives Conference, vol. 2, 2003, pp. 641–646.
[33] J. Larminie, J. Lowry, Electric Vehicle Technology Explained, Wiley, 2003.
[34] W. Leonhard, Control of Electrical Drives, second ed., Springer, 2001.
[35] C.-M. Ong, Dynamic Simulation of Electric Machinery, Prentice Hall, 1998.
[36] C.L. Chu, M.C. Tsai, H.Y. Chen, Torque control of brushless DC motors applied to electric vehicles, in: Electric Machines and Drives Conference, 2001, pp. 82–87.
[37] S. Skogestad, Simple analytic rules for model reduction and PID controller tuning, Journal of Process Control 13 (2003) 291–309.